Microscopic Theory of Intrinsic Shear and Bulk Viscosities

Wokyung Sung

Department of Physics
State University of New York at Stony Brook
Long Island, New York 11794

John Karkheck

Department of Mechanical Engineering
State University of New York at Stony Brook
Long Island, New York 11794

G. Stell

Departments of Mechanical Engineering and Chemistry
State University of New York at Stony Brook
Long Island, New York 11794

Report #349
August 1980

ABSTRACT

A microscopic theory of intrinsic shear and bulk viscosities is given for a model of particles that interact with hard-sphere cores and weak long-range attraction. The approximation considered (the velocity chaos assumption of the Enskog theory) can be expected to yield quantitatively useful values for viscosities of the model solute-solvent system when the solute particles are not much larger than the solvent particles. Under solute-solvent mixing conditions of constant pressure and temperature we find that the intrinsic viscosities of a hard-sphere solute in a hard-sphere solvent can be positive or negative, depending upon size and mass ratios; for solute and solvent particles whose mass ratio equals their volume ratio, the intrinsic shear and bulk viscosities are always positive for solute size larger than solvent size, and negative for smaller solute size. For smaller solute size, this result is sensitive to change in mass ratio. The addition of solvent-solvent attraction is found to lower the intrinsic viscosities substantially; the addition of solute-solvent attraction raises it. Detailed quantitative analysis of these effects is given.

I. INTRODUCTION

In 1906, Einstein derived an expression for the shear viscosity of a dilute suspension of spherical particles in an incompressible fluid.[1] The derivation assumes the suspended particles to be large enough compared to the fluid particles so that the latter can be regarded as a homogeneous structureless continuum rather than a molecular solvent. The Einstein result can be expressed as

$$\eta = \eta_{10}\left(1 + \tfrac{5}{2}\,\xi_2\right) \tag{1-1}$$

where η is the shear viscosity of suspension, η_{10} is the pure-fluid viscosity, ξ_2 the volume fraction of the suspended particles, i.e. the ratio of the total volume of the suspended particles to the total volume of the suspension.

This important result has been generalized to higher particle concentration and to nonspherical shapes.[2] To our knowledge, however, very little has been done toward generalizing the Einstein result to the case of a bona-fide molecular solvent of particles into which solute particles of molecular size have been introduced.[3] It is this case that we consider here.

We take as our Hamiltonian model a binary fluid of particles interacting pairwise with hard-sphere repulsion plus weak, long-range attraction. Our results are developed on the basis of the revised Enskog theory (RET) of hard-sphere mixtures[4] suitably extended to accommodate the attractive tail of the intermolecular potential. The relevant extension has recently been put on a firm

conceptual foundation by Karkheck and Stell.[5] The standard Chapman-Enskog procedure[6] is used to obtain the transport coefficients. In comparing the pure-solvent transport properties to those in the presence of solute, we are mainly interested in our system under the thermodynamic conditions that are usually easiest to handle in the laboratory--fixed temperature and external pressure. The key thermodynamic input needed in our calculation is provided by the equation of state for a binary mixture of hard spheres, which is modified in a simple way by the presence of the attractive tail. We use the equation of state of Mansoori et al.[7] (for hard spheres), which is known to be an extremely accurate approximation.

Although by no means exact, the resulting theory can be expected to yield with reasonable accuracy all the trends of the intrinsic shear and bulk viscosities for monoatomic fluids that we wish to study as long as the size and mass disparities are not too large. However, we cannot expect the Enskog result to remain meaningful in the hydrodynamic limit, i.e. the limit $q \to 0$ with solvent density fixed, where q is the ratio of the diameter of the solvent particle to that of solute. The Enskog theory assumes the "velocity chaos," i.e. the lack of dynamic correlation between two particles about to collide, and this assumption prevents an adequate description of certain collective effects involving repeated collisions that appear to be fundamental to the hydrodynamic description. As a result, the Enskog theory yields intrinsic

viscosities that become spuriously singular as $q \to 0$, as we shall see. In this paper we therefore focus mainly on the values of q not too much less than unity, for which Enskog theory can be expected to be most useful. We also restrict our attention to values of a_{ij}, the integrated strength of the attractive potential, that corresponds to values for simple mixtures that have been determined from the available thermodynamic data.

The presentation of our work is as follows: In sec. II, we give a brief sketch of our calculation of the intrinsic shear and bulk viscosities from the (revised) Enskog theory of hard spheres. A mixing rule for fixed temperature and pressure is derived. In sec. III we discuss how the inclusion of an infinitely weak, long-ranged attraction between pairs of molecules perturbs the results of pure hard-core repulsion. This is found to yield a nonnegligible contribution to the intrinsic quantities under our thermodynamic mixing condition. In sec. IV we give quantitative results and a discussion.

II. ENSKOG THEORY OF THE INTRINSIC SHEAR AND BULK VISCOSITIES FOR HARD-SPHERE FLUID

For the case of a dense fluid consisting of hard-spheres, the most successful microscopic theory capable of yielding useful analytic expressions for the transport coefficients is the kinetic theory of Enskog.[6] Since the collision time in this impulsive model is vanishingly small, the ternary and higher order collisions can be completely neglected, simplifying the collision kinematics considerably. While taking into account the static correlation existing from the finite dimension of the molecule, this theory neglects all the correlated collision events in its assumption of "velocity chaos." This assumption is expressed by the condition

$$F^{(2)}(\underset{\sim}{r}_1,\underset{\sim}{V}_1,\underset{\sim}{r}_2,\underset{\sim}{V}_2;t) = g_{12}(\underset{\sim}{r}_1,\underset{\sim}{r}_2)f_1(\underset{\sim}{r}_1,\underset{\sim}{V}_1,t)f_2(\underset{\sim}{r}_2,\underset{\sim}{V}_2,t) \tag{2-1}$$

which relates the two-particle distribution function (DF) $F^{(2)}(\underset{\sim}{r}_1,\underset{\sim}{V}_1,\underset{\sim}{r}_2,\underset{\sim}{V}_2;t)$ to the one-particle DF $f_i(\underset{\sim}{r}_i,\underset{\sim}{V}_i,t)$. In the standard (original) Enskog theory[6,8] (SET) g_{12} is the contact equilibrium pair DF which depends on the local density evaluated midway between the centers of the two molecules located at $\underset{\sim}{r}_1$, $\underset{\sim}{r}_2$. When applied to a mixture of disparate sizes, however, this prescription for g_{12} was found to lead to an inconsistency with the Onsager reciprocal relations.[9] Subsequently it was noted[4] that if one regards g_{12} as the local equilibrium DF which depends functionally on local density fields (just as it does at equilibrium in a system

made nonuniform by the presence of external fields), this treatment yields results that appear to be fully consistent with the reciprocal relations and are fundamentally more self-consistent and useful even for a pure fluid.[4,5,10] We shall use this new treatment [referred as the revised Enskog theory (RET)] as the starting point of our microscopic theory of transport in binary fluids. With regard to our final expressions for the shear and bulk viscosities, however, we note that there would be no differences had we used instead the SET as our starting point.

The kinetic equation given by the RET is

$$\left(\frac{\partial}{\partial t} + \underset{\sim}{V}_i \cdot \underset{\sim}{\nabla}\right) f_i(\underset{\sim}{r}, \underset{\sim}{V}_i, t) = \sum_{j=1,2} J_E(f_i f_j)$$

$$J_E(f_i f_j) = \sigma_{ij}^2 \int d\underset{\sim}{V}_j \int d\underset{\sim}{\sigma}\, (\underset{\sim}{\sigma} \cdot \underset{\sim}{V}_{ji}) \Theta(\underset{\sim}{\sigma} \cdot \underset{\sim}{V}_{ji})$$

$$\{g_{ij}(\underset{\sim}{r}, \underset{\sim}{r} + \sigma_{ij}\underset{\sim}{\sigma}) f_i(\underset{\sim}{r}, \underset{\sim}{V}_i', t) f_j(\underset{\sim}{r} + \sigma_{ij}\underset{\sim}{\sigma}, \underset{\sim}{V}_j', t)$$

$$- g_{ij}(\underset{\sim}{r}, \underset{\sim}{r} - \sigma_{ij}\underset{\sim}{\sigma}) f_i(\underset{\sim}{r}, \underset{\sim}{V}_i, t) f_j(\underset{\sim}{r} - \sigma_{ij}\underset{\sim}{\sigma}, \underset{\sim}{V}_j, t)\}. \qquad (2\text{-}2)$$

Here, σ_{ij} is the contact distance between the centers of the particles i and j, $\underset{\sim}{V}_{ji} = \underset{\sim}{V}_j - \underset{\sim}{V}_i$, the primes on the velocities denote the post collisional values, $\underset{\sim}{\sigma}$ is unit vector along the apse line in such a direction that Heaviside step function $\Theta(\underset{\sim}{\sigma} \cdot \underset{\sim}{V}_{ji})$ imposes the condition of the collision.

The hydrodynamic equation for change of mass, momentum, energy can be constructed from (2-2) by multiplying by m_1, $m_i \underset{\sim}{V}_i$, $\frac{1}{2} m_i V_i^2$, respectively, integrating with respect to $\underset{\sim}{V}_i$ and summing over i = 1,2.

Since our interest here lies in the viscosities, only the equation for the change of momentum is considered:

$$\rho\left(\frac{\partial \underset{\sim}{u}}{\partial t} + \underset{\sim}{u}\cdot\nabla\underset{\sim}{u}\right) = -\nabla\cdot\underset{\approx}{P} \tag{2-3}$$

where the hydrodynamic variables ρ, $\underset{\sim}{u}$, $\underset{\approx}{P}$ (mass density, velocity, pressure tensor, respectively) are defined through the relations

$$\rho = \sum_{i=1,2} \int f_i m_i d\underset{\sim}{V}_i \tag{2-4}$$

$$\rho\underset{\sim}{u} = \sum_{i=1,2} \int f_i m_i \underset{\sim}{V}_i d\underset{\sim}{V}_i \tag{2-5}$$

$$\underset{\approx}{P} = \underset{\approx}{P}_K + \underset{\approx}{P}_C$$

$$\underset{\approx}{P}_K = \sum_{i=1,2} \int f_i m_i (\underset{\sim}{V}_i - \underset{\sim}{u})(\underset{\sim}{V}_i - \underset{\sim}{u}) d\underset{\sim}{V}_i \tag{2-6}$$

$$\underset{\approx}{P}_C = \sum_{i,j=1,2} \sigma_{ij}^3 \mu_{ij} \int d\underset{\sim}{V}_j d\underset{\sim}{V}_i d\underset{\sim}{\sigma}\Theta(\underset{\sim}{\sigma}\cdot\underset{\sim}{V}_{ji})(\underset{\sim}{\sigma}\cdot\underset{\sim}{V}_{ji})^2 \underset{\sim}{\sigma}\underset{\sim}{\sigma}$$
$$\int_0^1 d\alpha\, g_{12}(\underset{\sim}{r} - \alpha\sigma_{ij}\underset{\sim}{\sigma},\ \underset{\sim}{r} - \alpha\sigma_{ij}\underset{\sim}{\sigma} + \sigma_{ij}\underset{\sim}{\sigma})$$
$$f_i(\underset{\sim}{r} - \alpha\sigma_{ij}\underset{\sim}{\sigma},\ \underset{\sim}{V}_i, t) f_j(\underset{\sim}{r} - \alpha\sigma_{ij}\underset{\sim}{\sigma} + \sigma_{ij}\underset{\sim}{\sigma}, \underset{\sim}{V}_j, t) \tag{2-7}$$

In (2-7) $\underset{\approx}{P}_C{}^{11}$ is identified as the collisional momentum transfer not included in the Boltzman-equation description. To evaluate $\underset{\approx}{P}$, one should solve for f_i. The Chapman-Enskog procedure of normal solution for f_i is known to provide an adequate means of yielding the hydrodynamic transport coefficients. We shall not elaborate here this standard procedure in detail but quote the results developed elsewhere.[8, 12] For $\underset{\approx}{P}$, we find up through linear order in gradient in the hydrodynamic velocity $\underset{\sim}{u}$

$$\underset{\approx}{P} = P\underset{\approx}{I} - \eta\left(\nabla\underset{\sim}{u} + (\nabla\underset{\sim}{u})^{+} - \tfrac{2}{3}\nabla\cdot\underset{\sim}{u}\underset{\approx}{I}\right) - \kappa\nabla\cdot\underset{\sim}{u} \ . \tag{2-8}$$

Thus, with this constitutive relation, (2-3) becomes the Navier-Stokes equation with η, κ the shear and bulk viscosities, now given microscopically. The η, κ are given by

$$\eta = \eta_1 + \eta_2 + \eta_3 \tag{2-9}$$

$$\eta_1 = \tfrac{1}{2}kT \sum_{i=1,2} n_i b_0^{(i)}$$

$$\eta_2 = \frac{4\pi kT}{15} \sum_{i,j=1,2} \frac{\mu_{ij}}{m_i} \beta_{ij}^{(3)} b_0^{(i)}$$

$$\eta_3 = \frac{4kT}{15} \sum_{i,j=1,2} p_{ij}\beta_{ij}^{(4)}$$

$$\kappa = \kappa_1 + \kappa_2 \tag{2-10}$$

$$\kappa_1 = \frac{4\pi kT}{3} \sum_{i,j=1,2} \frac{\mu_{ij}}{m_i} \beta_{ij}^{(3)} h_1^{(i)}$$

$$\kappa_2 = \frac{4kT}{9} \sum_{i,j=1,2} \beta_{ij}^{(4)} p_{ij}$$

Here $b_0^{(i)}$, $h_1^{(i)}$, the coefficients of the lowest order Sonine polynomial that is used in our approximation, are to be obtained from the conditions:

$$8 \sum_{j=1,2} \beta_{ij}^{(2)} p_{ij} \frac{\mu_{ij}}{m_i}\left(\frac{b_0^{(i)}}{m_i} + \frac{b_0^{(j)}}{m_j} - \frac{5}{3}\frac{b_0^{(j)} - b_0^{(i)}}{m_j}\right)$$

$$= 5n_i + \frac{8\pi}{3} \sum_{j=1,2} \beta_{ij}^{(3)} \frac{\mu_{ij}}{m_i} \tag{2-11}$$

$$8 \sum_{j=1,2} \beta_{ij}^{(2)} p_{ij} (h_1^{(j)} - h_1^{(i)}) M_{ij}^{-1}$$

$$= -n_i + \frac{n_i P}{nkT} + \frac{4\pi}{3} \beta_{ij}^{(3)} \frac{m_i}{M_{ij}} . \qquad (2\text{-}12)$$

The Y_{ij} is the contact value of the equilibrium pair distribution function, n_i is the number density of the species i, $n = n_1 + n_2$, $\mu_{ij} = m_i m_j / m_i + m_j$, $M_{ij} = m_i + m_j$, $\sigma_{ij} = \frac{1}{2}(\sigma_{ii} + \sigma_{jj})$, $\beta_{ij}^{(\ell)} = \sigma_{ij}^{\ell} n_i n_j Y_{ij}$, $p_{ij} = (2\pi kT\mu_{ij})^{\frac{1}{2}}$. For the pressure, we have

$$P = kT\left\{n + \frac{2\pi}{3} \sum_{i,j=1,2} \beta_{ij}^{(3)}\right\} . \qquad (2\text{-}13)$$

The calculations for the explicit η and κ are very tedious but straightforward. Since we shall concern ourselves with a suspension of dilute solute particles in which $\xi_1 >> \xi_2$ where $\xi_i = \frac{\pi}{6} n_i \sigma_{ii}^3$ is the volume fraction of the particle i, we expand η, κ up to the first order in ξ_2:

$$\eta = (\eta)_0 + \xi_2 (\eta)_1 \qquad (2\text{-}14)$$

$$(\eta)_0 = \left\{\frac{1}{Y_{11}^0}\left(1 + \frac{8}{5} \xi_1 Y_{11}^0\right)^2 + \frac{768}{25\pi} \xi_1^2 Y_{11}^0\right\} \eta^B$$

$$(\eta)_1 = \left\{\frac{1}{Y_{11}^0}\left(1 + \frac{8}{5} \xi_1 Y_{11}^0\right)\left\{\frac{2}{5}(1+q)^3\left(1 + \frac{\mu_{12}}{m_1}\right) Y_{12}^0 - \frac{Y_{11,2}^0}{Y_{11}^0} + \frac{8}{5} \xi_1 Y_{11,2}^0\right\}\right.$$

$$+ \left\{\frac{768}{25\pi} \xi_1^2 Y_{11,2}^0 + \frac{96}{25\pi}\left(\frac{2\mu_{12}}{m_1}\right)^{\frac{1}{2}} (1+q)^4 q^{-1} \xi_1 Y_{12}^0\right\}$$

$$+ \xi_1^{-1}\left(1 + \frac{2}{3} \frac{\mu_{12}}{m_1}\right)^{-1} \frac{1}{Y_{11}^0}\left(1 + \frac{8}{5} \xi_1 Y_{11}^0\right)\left\{\frac{2}{3} q^3 \frac{\mu_{12}}{m_1}\right.$$

$$\left. - \frac{5}{12} q(1+q)^2 \left(\frac{2\mu_{12}}{m_1}\right)^{\frac{1}{2}}\right.$$

$$\left.\times \frac{1}{Y_{11}^0}\left(1 + \frac{8}{5} \xi_1 Y_{11}^0\right) Y_{12}^0 + \frac{2}{5}\left(\frac{\mu_{12}}{m_1} - 1\right)(1+q)^3 \xi_1 Y_{12}^0\right\}$$

$$+ \xi_1^{-1}\left(1 + \frac{2}{3}\frac{\mu_{12}}{m_1}\right)^{-1}\left\{\frac{2}{3}\left(\frac{\mu_{12}}{m_1}\right)\frac{1}{Y_{11}^0}(1 + \frac{8}{5}\xi_1 Y_{11}^0)\right.$$

$$+ 4\left((1+q)^2\left(\frac{2\mu_{12}}{m_1}\right)^{\frac{1}{2}} pq\right)^{-1} Y_{12}^{0\,-1}\left(q^3 + \frac{2}{5}(1+q)^3 p\,\frac{\mu_{12}}{m_1}\,\xi_1 Y_{12}^0\right)\Big\}$$

$$\times \left(q^3 + \frac{2}{5}(1+q)^3 p\,\frac{\mu_{12}}{m_1}\,\xi_1 Y_{12}^0\right)\Big]\eta_1^B$$

$$\kappa = (\kappa)_0 + \xi_2(\kappa)_1 \tag{2-15}$$

$$(\kappa)_0 = \frac{256}{5\pi}\,\xi_1^2 Y_{11}^0 \eta_1^B$$

$$(\kappa)_1 = \left(\frac{256}{5\pi}\,\xi_1^2 Y_{11,2}^0 + \frac{32}{5\pi}\left(\frac{2\mu_{12}}{m_1}\right)^{\frac{1}{2}} q^{-1}(1+q)^4 \xi_1 Y_{12}^0\right.$$

$$\left. + \frac{4\sqrt{2}}{5}\left(\frac{\mu_{12}}{m_1}\right)^{-3/2}\left(pq(1+q)^2\right)^{-1} Y_{12}^0\left(q^3\,\frac{Y_{11}^0}{Y_{12}^0} - \frac{1}{4}(1+q)^3 p\,\frac{\mu_{12}}{m_1}\right)^2\right)\eta_1^B.$$

In (2-15) $p = m_1/m_2$, $q = \sigma_{11}/\sigma_{22}$, $\eta_1^B = \frac{5}{16}\left(\frac{m_1 kT}{\pi}\right)^{\frac{1}{2}}\frac{1}{\sigma_{11}^2}$

$$Y_{ij}^0 = Y_{ij}\Big|_{\xi_2=0},\quad Y_{ij,k}^0 = \frac{\partial}{\partial \xi_1} Y_{ij}\Big|_{\xi_2=0}.$$

For the pressure, we find

$$P = (P)_0 + \xi_2(P)_1 \tag{2-16}$$

$$(P)_0 = n_1 kT(1 + 4\xi_1 Y_{11}^0)$$

$$(P)_1 = n_1 kT\{4\xi_1 Y_{11,2}^0 + (1+q)^3 Y_{12}^0\}.$$

The viscosities and pressure in the pure solvent are obtained by substituting ξ_1^0, n_1^0, relevant to the pure solvent for ξ_1, n_1 in $(\eta)_0$, $(\kappa)_0$ and $(P)_0$:

$$\eta_{10} = \left(\frac{1}{Y_{11}^0(\xi_1^0)}\left\{1 + \frac{8}{5}\,\xi_1^0 Y_{11}^0(\xi_1^0)\right\}^2 + \frac{768}{25\pi}\,\xi_1^{0\,2} Y_{11}^0(\xi_1^0)\right)\eta_1^B \tag{2-17}$$

$$\kappa_{10} = \left(\frac{256}{5\pi}\,\xi_1^{0\,2} Y_{11}^0\,(\xi_1^0)\right)\eta_1^B \tag{2-18}$$

$$P_{10} = n_1^0 kT\{1 + 4\xi_1^0 Y_{11}^0(\xi_1^0)\}. \tag{2-19}$$

In order to compare the viscosities of the suspension with those of the pure solvent, the thermodynamic conditions of both systems should be specified. We shall assume, in mixing, fixed conditions of temperature, total solvent mass, and external pressure, which represents the most common experimental situation. To show how this condition differentiates ξ_1 from ξ_1^0, $Z = P/kT$ is expanded up through the deviation linear in ξ_2:

$$Z = Z_0 + \left(\frac{\partial Z}{\partial \xi_1}\right)_0 (\xi_1 - \xi_1^0) + \left(\frac{\partial Z}{\partial \xi_2}\right)_0 \xi_2 \tag{2-20}$$

where 0 refers to the pure solvent, i.e. the point ($\xi_1 = \xi_1^0$, $\xi_2 = 0$). By substituting the mixing rule in the form

$$\xi_1 = \xi_1^0(1 - M\xi_2) \tag{2-21}$$

and by noting that $Z = Z_0$, we find

$$M = \left(\frac{\partial Z}{\partial \xi_2}\right)_0 \Big/ \xi_1^0 \left(\frac{\partial Z}{\partial \xi_1}\right)_0 \tag{2-22}$$

$$= \left(\frac{\partial P}{\partial \xi_2}\right)_0 \Big/ \xi_1^0 \left(\frac{\partial P_{10}}{\partial \xi_1^0}\right).$$

Substituting (2-16), (2-19), we find for the hard-spheres

$$M_H = \frac{1}{\xi_1^0} \frac{q^3 + (1+q)^3 \xi_1^0 Y_{12} + 4\xi_1^{0\,2} Y_{11,2}^0}{1 + 8\xi_1^0 Y_{11}^0 + 4\xi_1^{0\,2} Y_{11,1}^0}. \tag{2-23}$$

This also can be expressed as

$$M = \beta_1^0 \left(\frac{\partial P}{\partial \xi_2}\right)_0. \tag{2-24}$$

where β_1^0 is the isothermal compressibility of pure solvent defined as

$$\beta_1^0 = -\frac{1}{V_0}\left(\frac{\partial V_0}{\partial P_{10}}\right)_T = \left(n_1^0 \frac{\partial P_{10}}{\partial n_1^0}\right)_T^{-1}. \qquad (2\text{-}25)$$

For the fluid of general intermolecular interaction, (2-24) will provide a means of determining M through thermodynamic measurements.

The simplest and most illuminating expression for M in the operational sense is simply given as follows: Consider a sample volume V_0 of the pure solvent. By adding an infinitesimally small amount of the solute particles, the overall volume also will generally increase infinitesimally (ΔV). The volume fraction of the solvent particles would be affected according to the relation

$$\xi_1 = \frac{N_1 v_1}{V_0 + \Delta V} = \xi_1^0\left(1 - \frac{\Delta V}{V_0}\right) \qquad (2\text{-}26)$$

where v_1, N_1 are the molecular volume and the total number of the solvent particle. By comparing this with (2-21), we find

$$M = \frac{\Delta V}{V_2} \qquad (2\text{-}27)$$

where $V_2 = N_2 v_2$ is the total volume of the solute mixed. Thus, determination of M requires only a simple experiment of measuring the volume overflow ΔV.

Let us imagine the case in which the solute particles are macroscopically large. Our macroscopic experience immediately tells us that $M_H = 1$ in this limit, since in hard-sphere repulsion there is no solvation effect, i.e. $V_2 = \Delta V$. In fact, when the Mansoori-Carnahan-Starling-Leland (MCSL)[7] approximation for Y_{ij} (see appendix) is used, (2-23) gives in this limit a value ranging from 0.98 to 1. This remarkable slight deviation from unity suggests strongly

the possibility that the MCSL remains a good approximation in the $q \to 0$ limit.

With the mixing rule (2-21), (2-23), we are now in a position to evaluate the intrinsic viscosities defined by[13]

$$\{\eta\} \equiv \lim_{\xi_2 \to 0} \frac{\eta - \eta_{10}}{\xi_2 \eta_{10}} \tag{2-28}$$

$$\{\kappa\} \equiv \lim_{\xi_2 \to 0} \frac{\kappa - \kappa_{10}}{\xi_2 \eta_{10}} \tag{2-29}$$

We find from (2-14) and (2-15)

$$\{\eta\} = -M_H \xi_1^0 \frac{1}{\eta_{10}} \frac{\partial (\eta)_0}{\partial \xi_1^0} + \frac{(\eta)_1}{\eta_{10}} \Bigg|_{\xi_1 = \xi_1^0}$$

$$= -M_H \xi_1^0 \frac{1}{\eta_{10}} \frac{\partial \eta_{10}}{\partial \xi_1^0} + \frac{(\eta)_1(\xi_1^0)}{\eta_{10}} \tag{2-30}$$

$$\{\kappa\} = -M_H \xi_1^0 \frac{1}{\eta_{10}} \frac{\partial \kappa_{10}}{\partial \xi_1^0} + \frac{(\kappa)_2(\xi_1^0)}{\eta_{10}} \, . \tag{2-31}$$

Figures 1 and 2 show trends in $\{\eta\}$ and $\{\kappa\}$ for the case $p^{-1} \equiv m_2/m_1 = (\sigma_{22}/\sigma_{11})^{\alpha}$ ($\alpha = 0,2,3,4$) for $\xi_1^0 = 0.4$, the volume fraction of the typical dense liquid. A remarkable feature, first of all, is the divergence that goes as $q^{-1} = \sigma_{22}/\sigma_{11}$ where $q = \sigma_{11}/\sigma_{22} \to 0$. Since in this limit the size of the solute particle is infinitely larger than the mean free path of the solvent molecules, we naturally expect the hydrodynamic description (in which the solvent is regarded as a structureless continuum on the length scale of the size of solute particle) to yield the exact result. Since the intermolecular force between the solute and solvent particles is a hard-sphere repulsion which lacks a tangential component, the macroscopic collective manifestation of the solute-

solvent interaction results in the form of slip boundary condition for the hydrodynamic variables on the surface of the solute particle. Hydrodynamic calculation with this boundary calculation yields $\{\eta\} = 1$, $\{\kappa\} = 4/3 + \kappa/\eta$.[14] (The famous Einstein formula $\{\eta\} = 5/2$ will only result from an anisotropic molecular interaction that allows transfer of angular momentum at collision, permitting the usual stick boundary condition.)

The reason for this pathological divergence in our kinetic theory calculation is due to the velocity chaos assumption that breaks down badly in this limit, in which the solvent particles near to the large solute particle are likely to make repeated (correlated) collisions with it. The resulting singularity (q^{-1}) in $\{\eta\}$, $\{\kappa\}$ is similar to that which appears in the Enskog binary diffusivity, in comparison with the hydrodynamic (Stokes-Einstein) result.

However, in the region of very large q, in which the average spacing between the solvent particles is far larger than the size of the solute particle (and thus the solute-solvent collision tends to be uncorrelated) one might expect the velocity-chaos assumption for the solute-solvent collision to better retain its validity. This tendency has been verified in the case of binary diffusion through molecular dynamics studies.[15] This tendency and the fact that the Enskog results satisfy the exact symmetry conditions that force $\{\eta\}$ and $\{\kappa\}$ to vanish at $q = 1 = p$ strongly suggest that Fig. 1 and Fig. 2 represent the trends of $\{\eta\}$, $\{\kappa\}$ for hard-spheres with reasonable accuracy in the region $q^{-1} \lesssim 1$, i.e. the region where the

aforementioned singularity (q^{-1}) is not appreciable. In addition to the Enskog approximation embedded in Eqs. (2-14), (2-15), and Figs. 1 and 2 one has the approximations introduced in getting the transport coefficients from the Enskog equation. The Chapman-Enskog method of normal solution that we use seems to be appropriate in our study of transport coefficients as long as the mixture can be regarded as homogeneous in the local temperature and hydrodynamic velocity. It remains only to show how our results (2-14), (2-15) based on the lowest Sonine polynomial approximation can remain acceptable in this limit; this is presently under our investigation.

In the intermediate region of q, $\{\eta\}$ and $\{\kappa\}$ must vanish at the point $q = 1 = p$, which is no more than a statement of identity of two species. Inclusion of molecules identical to those of the solvent under constant pressure and temperature does not affect the property of the initial system.

Finally we note from Figs. 1 and 2 that our way of classifying the mixture via $p = q^{\alpha}$, albeit somewhat artificial, shows how the intrinsic viscosities are sensitive to the mass ratio. As one might expect, the result is more insensitive to the mass ratio (i.e. the solute-solvent collisional detail) for the larger solute particle; we find for all values α in the domain $1 < \alpha < 5$ the results approach a single asymptote in the limit $q \to 0$. In the opposite limit, however, the result is very sensitive to the mass ratio.

III. INCLUSION OF THE INFINITELY WEAK AND LONG-RANGED ATTRACTION

It is well-known that the hard-sphere model, though crude, represents the main features of the dense fluid structure and is successful in correlating the data of the transport coefficients of real dense fluids in various ways.[17] These facts lend support to the view that a workable perturbation theory of the transport can be developed with hard-sphere fluid taken as a reference system. This scheme has already produced fruitful results in regard to thermodynamic properties.

We shall consider here the perturbation in the form of the weak and long-ranged attraction (van der Waal's attraction) added to the hard-core repulsion. The intermolecular potential is written as

$$\phi(r) = \phi_H + \gamma^3 \phi_L(\gamma r) \tag{3-1}$$

where the smallness parameter γ is the inverse of the range of the attractive force.

Resibois et al.[18] discovered that the leading effect of the perturbation on the shear and bulk viscosities is only in the order of γ:

$$X(\gamma) = X_H + O(\gamma). \tag{3-2}$$

Thus, the transport coefficients are those of the hard-sphere reference system in the limit $\gamma \to 0$. However, as is well known, the thermodynamic properties are different in a significant way:[19] For the free energy and pressure we have

$$A = A_H + an^2/kT \tag{3-3}$$

$$p = p_H - an^2 \tag{3-4}$$

where

$$-2a = \lim_{\gamma \to 0} \gamma^3 \int_{\sigma_{11}}^{\infty} \phi_L(\gamma r) d\underset{\sim}{r} \tag{3-5}$$

$$= \int_0^{\infty} \phi_L(x) d\underset{\sim}{x}$$

but for the radial distribution functions at its contact value, we get

$$Y_{12}(\sigma_{12}) = Y_{12}^{\grave{H}}(\sigma_{12}) + O(\gamma^3). \tag{3-6}$$

With the hard-sphere pressure P_H given by the Percus-Yevick compressibility expression or by the more exact form of Carnahan and Starling[20] (see appendix), (3-4) is a modified van der Waals equation of state which yields reasonable thermodynamics for the monatomic fluids.[21]

The generalization of (3-5) to binary mixtures is achieved by the van der Waals prescription[22]

$$n^2 a = \sum_{i,j=1,2} n_i n_j a_{ij} \tag{3-7}$$

where

$$-2a_{ij} = \lim_{\gamma \to 0} \gamma^3 \int_{\sigma_{ij}}^{\infty} \phi_i^{ij}(\gamma r) d\underset{\sim}{r} \tag{3-8}$$

$$= \int_0^{\infty} \phi_L^{ij}(x) d\underset{\sim}{x}$$

and by (2-13)

$$P_H/kT = n + \frac{2\pi}{3} \sum_{i,j} n_i n_j \sigma_{ij}^3 Y_{ij}.$$

In our calculation of the excess transport properties, the inclusion of the perturbation is expected to give a significant contribution, via our thermodynamic mixing function M (2-21). From (2-22), (2-16), (2-19) we find

$$M = M^H + \Delta M$$

$$= \frac{1}{\xi_1^0} \frac{q^3+(1+q)^3\xi(Y_{12}^0-b_{12})+4\xi_1^{0\,2}Y_{11,2}^0}{1+8\xi_1^0(Y_{11}^0-b_{11})+4\xi_1^{0\,2}Y_{11,1}^0} \qquad (3\text{-}9)$$

where $b_{ij} = \frac{3}{2\pi} a_{ij} \sigma_{ij}^{-3}/kT$. The intrinsic viscosities are obtained by replacing M_H by this M in the expression (2-30), (2-31). In the case that two components are identical, i.e. $q = 1$, $b_{11} = b_{12} = b_{22}$, we find

$$M = M^H = \frac{1}{\xi_1^0} .$$

However, if the two species are identical in mass and size but internally dissimilar in such a way that $a_{11} \neq a_{12}$, ΔM does not vanish. Specifically when $a_{11} > a_{12}$, we have $\Delta M > 0$, and the mixing results in a decrease of the viscosities by $-\Delta M \xi_1^0 \frac{1}{X_{10}} \frac{\partial X_{10}}{\partial \xi_1^0}$. In the opposite case, the opposite result will be found. These results are intuitively obvious--the increase of the attraction by mixing ($a_{11} < a_{12}$) increases the viscosities.

Determination of a_{ij}.

The expressions (3-3) - (3-8) do not yield a unique means of finding a_{ij} and σ_{ij} that are appropriate to the study of real fluids, since real fluids do not have thermodynamics precisely given by these equations. Procedures to find a_{ij} and σ_{ij} that yield

reasonable approximations to the true thermodynamics are well known, however. We shall use the values of a_{ij} and σ_{ij} that were determined by Snider and Herrington[23] from thermodynamic data for simple binary mixtures composed of the almost spherical molecules. They made their determination first for pure fluids by comparing thermodynamic data (PVT) and the latent heat of vaporization, with the equation (3-4) and the expressions for the molar entropy or enthalpy of vaporization that they obtained. In order to obtain a_{12}, they matched their expressions for the excess Gibbs free energy with the measured data. With these semi-empirical values of a_{ij}, σ_{ij}, they predicted the excess enthalpy and entropy of mixtures with successful agreement with the measured data.

Snider and Herrington used the Percus-Yevick hard sphere equation of state to evaluate the hard sphere term P_H in (3-4), rather than the slightly more accurate MCSL result[7] used by us, but this can be expected to make a negligible difference in the values of a_{ij} and σ_{ij}. Such fine points are inconsequential to our goal of determining the general trends that will result from the inclusion of attractive potentials that are of the same order of integrated strength as those found in typical fluid mixtures.

V. RESULTS AND DISCUSSION

Summing up the contributions from the Enskog result for hard-spheres and from the weak and long-range attraction, we have

$$\{X\} = \{X_E\} + \Delta\{X\}_a$$

$$= -\frac{1}{X_{10}}\left(\frac{\partial X_{10}}{\partial \xi_1^0}\right) M\xi_1^0 + \frac{(X)_1}{X_{10}} \qquad (4\text{-}1)$$

where X is either η or κ.

In table I and II we list the parameters a_{ij}, σ_{ij} determined by Sneider and Herrington. In general the diameters σ_{ii} given here are a little smaller than the effective diameters determined by other means.[24] Our results at $\xi_1^0 = 0.4$ are given in table III for the various mixtures considered by Sneider and Herrington. As is shown, $\Delta\{\eta\}_a$, $\Delta\{\kappa\}_a$ are appreciable and in many cases predominate over the $\{\eta\}_E$, $\{\kappa\}_E$.

Figure 3 shows the trends in $\Delta\{\eta\}_a$ and $\Delta\{\kappa\}_a$ $(\Delta\{\eta\}_a = 0.7794\ \Delta\{\kappa\}_a)$ for mixing of the solute particles of various sizes and strength a_{12} into the reference fluid of argon at T = 100 K. For simplicity, we consider the case $m_2/m_1 = (\sigma_{22}/\sigma_{11})^3$, i.e. the case in which the molecular mass density of the solute and solvent are the same, with the trends plotted for various values of fixed attractive solute-solvent (argon) strength a_{12}. Figures 4 and 5 represent the general trends of $\{X\}_E + \Delta\{X\}_a$. We know of no controllable physical process corresponding to changing the size of the solute particle while holding its attractive solute-solvent interaction strength fixed. Presumably one might be able to

experimentally locate a family of solute molecule of different sizes but with roughly the same attractive solute-solvent strength; without such a family with which to compare, Figs. 3, 4 and 5 remain somewhat physically artificial. Nevertheless they are conceptually extremely illuminating. Since the effect of dynamic correlation that Enskog theory neglects is not considered here, the reliability of the results of Figs. 4 and 5 is limited to the case of small solute particles, i.e. $\sigma_{22}/\sigma_{11} \lesssim 1$. However, as far as the $\Delta\{X\}_a$ themselves are concerned Fig. 3 can be regarded as representing with reasonable accuracy the effect of the attraction, since the inclusion of the infinitively weak, long-range attractive tails does not change the nature of the hard sphere collision dynamics. As is shown in Figs. 3, 4 and 5, the presence of the attractive tails perturbs the general trends of $\{X\}$ drastically. If we add only solvent-solvent attraction ($a_{11} > 0$) of strength typical of simple molecules but no solute-solvent attraction [$a_{12} = 0$ the graphs labelled by (0)] to the pure hard-sphere case (shown by the dashed lines), then the intrinsic shear and bulk viscosities are substantially lowered by values that are essentially independent of σ_{22}/σ_{11} once this ratio exceeds three or so; they respectively approach 4.27 and 5.49 asymptotically as $\sigma_{22}/\sigma_{11} \to \infty$. When we turn on the solute-solvent attraction in addition ($a_{12} > 0$) with a_{12} comparable to a_{11}, appreciable change occurs only for σ_{22}/σ_{11} less than 3, where the solute-solvent attraction keeps the intrinsic viscosities from becoming extremely negative [as they become when σ_{22}/σ_{11} decreases

below unity in the absence of the solute-solvent interaction; graphs labelled by (0)]. For $a_{12}/a_{11} \gtrsim 1$, in fact, $\{\eta\}$, $\{\kappa\}$ rapidly increase as σ_{22}/σ_{11} decreases past unity, while higher solute-solvent attraction (e.g. $a_{12}/a_{11} \gtrsim 15$) is enough to keep $\{\eta\}$, $\{\kappa\}$ positive for all σ_{22}/σ_{11}. This feature is expected to remain unchanged even if we were to include the effect of the dynamic correlation left out of the Enskog theory and thus eliminate the singular linear rise proportional to σ_{22}/σ_{11} as σ_{22}/σ_{11} goes to infinity. As this limit is approached with a_{12} fixed, we observe that the effect of the solute-solvent attraction disappears and thus $\{X\}$ approaches its value for the case $a_{12} = 0$. This is not surprising, since a_{12} would have to grow along with σ_{12} in order to maintain a nonvanishing effect on the transport as $\sigma_{22}/\sigma_{11} \to \infty$. We note that the method of determining M via direct measurement of $\Delta V/V_2$ (2-27) may be the best way of gaining experimental mixing-rule information in finding $\Delta\{X\}_a$ when the values of a_{ij} for mixture under consideration have not already been inferred from other studies.

Since they do not include the effect of dynamic correlation, the Enskog results for $\{X\}$ can be expected to depart from the true results at high values of σ_{22}/σ_{11} and at high solvent density. We shall come back to this problem of correcting the Enskog theory in the following paper.[14]

ACKNOWLEDGMENTS

G. Stell acknowledges the Office of Basic Energy Sciences, Department of Energy, and W. Sung acknowledges the National Science Foundation, for support of their research. J. Karkheck acknowledges both the above agencies, as well as the Donors of the Petroleum Research Fund, administered by the American Chemical Society, for support of his research.

APPENDIX

Mansoori-Carnahan-Starling-Leland (MCSL) approximation for Y_{ij}.[7]

$$Y_{11} = (1-\xi)^{-1} + \frac{3}{2}(1-\xi)^{-2}(\xi_1 + q\xi_2) + \frac{1}{2}(1-\xi)^{-3}(\xi_1 + q\xi_2)^2$$

$$Y_{12} = (1-\xi)^{-1} + 3(1+q)^{-1}(1-\xi)^{-2}(\xi_1 + q\xi_2) + 2(1+q)^{-2}(\xi_1 + q\xi_2)^2$$

$$Y_{22} = (1-\xi)^{-1} + \frac{3}{2}\, q^{-1}(1-\xi)^{-2}(\xi_1 + q\xi_2) + \frac{1}{2}\, q^{-2}(\xi_1 + q\xi_2)^2$$

where

$$\xi = \xi_1 + \xi_2$$

$$\xi_i = \frac{\pi}{6}\, n_i \sigma_{ii}^3$$

$$q = \sigma_{11}/\sigma_{22}$$

At $q = 1$, Y_{ij} is reduced to the Carnahan-Starling Y_{11} of one-component fluid, which yields the exact equation of state. When the last terms of the above expressions are truncated, they are reduced to the Percus-Yevick Y_{ij}.

REFERENCES

1. A. Einstein, Ann. Phys. 19, 289 (1906); 34, 591 (1911).

2. J. Peterson, M. Fixman, J. Chem. Phys. 39, 2516 (1963).

   G. K. Batchelor, J. T. Green, J. Fluid Mech. 56, 401 (1972).

   D. Bedeaux, R. Kapral, P. Mazur, Physica 88 A, 88 (1977).

   G. B. Geoffery, Proc. Roy. Soc. (London) A 102, 161 (1922).

3. The only previous statistical mechanical study yielding explicit analytic and quantitative results of which we are aware is the interesting exploratory investigation of a hard-sphere system by W. A. McElhannon and E. McLaughlin, Mol. Phys. 36, 967 (1978). Their calculations were made without the use of a physically realistic solute-solvent mixing condition, which has important numerical consequences. In addition, we find some calculational mistakes in their work.

4. H. Van Beijeren, M. H. Ernst, Physica 68, 437 (1973); 70, 225 (1973).

5. J. Karkheck and G. Stell, CEAS Report #350 (Sept. 1980).

6. S. Chapman, T. G. Cowling, The Mathematical Theory of Nonuniform Gases (Cambridge University Press, Cambridge, England, 1952).

7. G. A. Mansoori, N. F. Carnahan, K. E. Starling, T. W. Leland, J. Chem. Phys. 54, 1523 (1971).

8. M. K. Tham, K. E. Gubbins, J. Chem. Phys. 55, 268 (1971).

9. L. Barajas, L. S. Garcia-Colin, E. Piña, J. Stat. Phys. 7, 1961 (1973).

10. P. Resibois, Phys. Rev. Lett. 40, 1409 (1978); Physica 94A, 1 (1978).

11. J. T. O'Toole, J. S. Dahler, J. Chem. Phys. 32, 1097 (1960).

12. H. H. Thorne, see Ref. 6, Chap. 16.

J. Karkheck, G. Stell, J. Chem. Phys. 71, 3636 (1979).

13. Our definition of the intrinsic shear viscosity is nondimensional and thus different from the conventional one which carries the dimension of inverse mass density:

$$[\eta] = \lim_{c_2 \to 0} \frac{\eta - \eta_{10}}{c_2 \eta_{10}}$$

where $c_2 = n_2 m_2$. We also define the intrinsic bulk viscosity in terms of η_{10} rather than κ_{10}, since κ_{10} vanishes in the low density limit.

14. W. Sung, G. Stell (to appear).

15. B. J. Alder, W. E. Alley, J. H. Dymond, J. Chem. Phys. 61, 1415 (1974).

16. D. Chandler, Acc. Chem. Res. 7, 246 (1974).

17. J. H. Dymond, B. J. Alder, J. Chem. Phys. 45, 2061 (1966).

J. H. Dymond, Physica A 75, 100 (1974).

18. J. Piasecki, R. Resibois, J. Math. Phys. 14, 1984 (1973).

R. Resibois, J. Piasecki, Y. Pomeau, Phys. Rev. Lett. 28, 882 (1972).

19. M. Kac, G. Uhlenbeck, P. C. Hemmer, J. Math. Phys. 4, 216, 229 (1963); 5, 60 (1964).

J. L. Lebowitz, G. Stell, S. Baer, ibid. 4, 1382 (1964).

20. N. F. Carnahan, K. E. Starling, J. Chem. Phys. 51, 635 (1969).

21. H. C. Longuet-Higgins, B. Widom, Mol. Phys. 8, 549 (1964).

22. J. D. van der Waals, Z. Physik. Chem. 5, 133 (1890).

23. N. S. Snider, T. M. Herrington, J. Chem. Phys. 47, #7, 2248 (1967).

24. L. Verlet, Phys. Rev. 159, 98 (1967).

Table I. The Snider-Herrington parameters for a pure component.

	mass (atomic units)	diameters (10^{-8}cm)	a_{11} (10^{-36}cm^{3}erg)
Ar	39.94	3.356	4.58
Kr	83.80	3.583	7.69
N_2	28.02	3.560	4.74
O_2	32.00	3.338	4.69
CO	28.01	3.597	5.24
CH_4	16.04	3.701	7.72

Table II. The Snider-Herrington a_{12} (10^{-36}cm^{3}erg)

$Ar+K_2$	5.876	$Ar+N_2$	4.662
$Ar+O_2$	4.852	Ar+CO	4.821
N_2+O_2	4.74	N_2+CO	4.840
$CO+CH_4$	6.23	$Kr+CH_4$	7.271

Table III. Intrinsic shear and bulk viscosities of simple mixtures at the solvent (species 1) volume fraction $\xi_1^0 = 0.4$ and at temperatures a) 100 K b) 150 K c) 200 K $\Delta\{\eta\}_a$ and $\Delta\{\kappa\}_a$ are the contributions from the attractive tails of the interparticle potentials

Species 1	Species 2	$q = \frac{\sigma_{11}}{\sigma_{22}}$	$p = \frac{m_1}{m_2}$	$\{\eta\}_E$	$\Delta\{\eta\}_a$	$\{\kappa\}_E$	$\Delta\{\kappa\}_a$
Ar	Kr	0.937	0.477	0.898	[a] 1.179	1.138	1.513
					[b] 0.540		0.693
					[c] 0.350		0.449
Kr	Ar	1.068	2.098	-1.201	[b] -1.202	-1.705	-1.542
					[c] -0.703		-0.902
Ar	N_2	0.943	1.426	-0.314	[a] -1.061	-0.118	-1.361
					[c] -0.315		-0.404
N_2	Ar	1.061	0.701	0.319	[a] 0.942	0.418	1.209
					[c] 0.314		0.403
Ar	O_2	1.005	1.248	-0.297	[a] 0.125	-0.283	0.160
					[c] 0.037		0.047
O_2	Ar	0.995	0.801	0.278	[a] -0.410	0.305	-0.526
					[c] -0.117		-0.150
Ar	CO	0.993	1.426	-0.290	[a] -0.948	-0.369	-1.216
					[c] -0.281		-0.361
CO	Ar	1.072	0.701	0.300	[a] 0.612	0.411	0.785
					[c] 0.194		0.249
Ar	CH_4	0.907	2.490	-0.919	[a] 0.299	-0.239	0.384
					[c] 0.089		0.114
CH_4	Ar	1.103	0.402	0.875	[b] -0.635	1.853	-0.815
					[c] -0.386		-0.495

Table III (continued)

Species 1	Species 2	$q = \frac{\sigma_{11}}{\sigma_{22}}$	$p = \frac{m_1}{m_2}$	$\{\eta\}_E$	$\Delta\{\eta\}_a$	$\{\kappa\}_E$	$\Delta\{\kappa\}_a$
N_2	O_2	1.067	0.876	0.030	[a] 1.225 [c] 0.408	0.013	1.572 0.523
O_2	N_2	0.938	1.142	-0.028	[a] -1.337 [c] -0.381	0.100	-1.715 -0.489
N_2	CO	0.990	1.000	0.021	[a] 0.160 [c] 0.053	0.034	0.205 0.068
CO	N_2	1.010	1.000	-0.021	[a] -0.336 [c] -0.106	-0.033	-0.431 -0.136
CO	CH_4	0.972	1.746	-0.655	[a] 1.062 [c] 0.336	-0.441	1.363 0.431
CH_4	CO	1.029	0.573	0.596	[b] -1.105 [c] -0.672	0.808	-1.418 -0.862
Kr	CH_4	0.968	5.224	-2.026	[b] -1.036 [c] -0.605	-0.917	-1.329 -0.776
CH_4	Kr	1.033	0.191	1.528	[b] 0.052 [c] 0.032	4.201	0.067 0.041

FIGURE CAPTIONS

Figure 1. Intrinsic shear viscosity vs. σ_{22}/σ_{11} at solvent volume fraction $\xi_1^0 = 0.4$. The case $m_2/m_1 = (\sigma_{22}/\sigma_{11})^3$ is denoted by a solid line, the case $m_1 = m_2$ by a dashed line, the case $m_2/m_1 = (\sigma_{22}/\sigma_{11})^2$ by open circles, and the case $m_2/m_1 = (\sigma_{22}/\sigma_{11})^4$ by crosses.

Figure 2. Intrinsic bulk viscosity vs. σ_{22}/σ_{11} at solvent volume fraction $\xi_1^0 = 0.4$. Conditions and notations as in Fig. 1.

Figure 3. Contribution of intermolecular attraction to $\{\eta\}$ and $\{\kappa\}$ expressed in terms of $\Delta\{\eta\}_a = 0.78\ \Delta\{\kappa\}_a$ for the case $m_2/m_1 = (\sigma_{22}/\sigma_{11})^3$, $\xi_1^0 = 0.4$. The numbers in parentheses indicate the ratio a_{12}/a_{11}.

Figure 4. $\{\eta\}_E + \Delta\{\eta\}_a$ vs. σ_{22}/σ_{11}. Conditions and notations as in Fig. 3. The dashed line represents $\{\eta\}_E$.

Figure 5. $\{\kappa\}_E + \Delta\{\kappa\}_a$ vs. σ_{22}/σ_{11}. Conditions and notations as in Fig. 3. The dashed line represents $\{\kappa\}_E$.

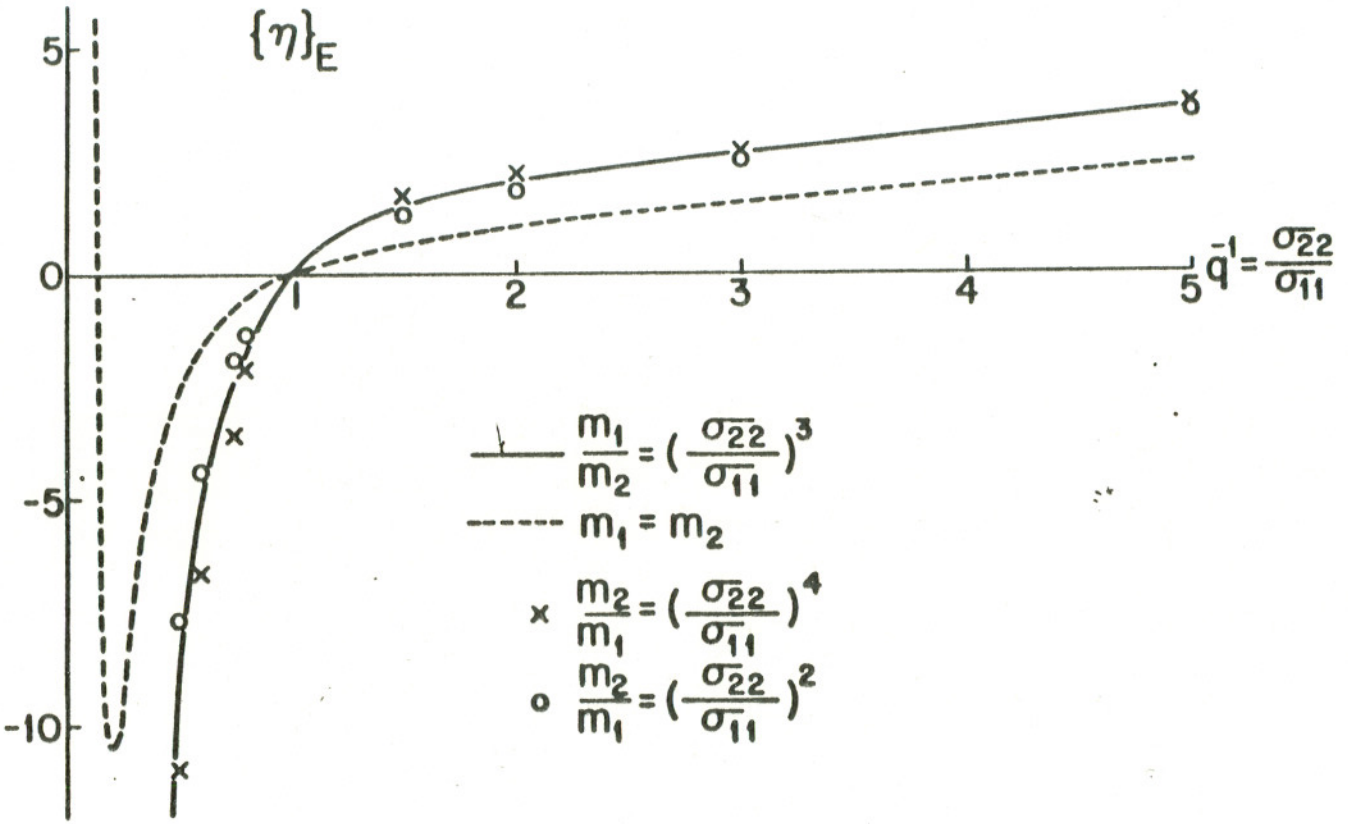
$\{\eta\}_E$
5
0
-5
-10
1
2
3
4
5
$\bar{q}^1 = \frac{\sigma_{22}}{\sigma_{11}}$
$\frac{m_1}{m_2} = (\frac{\sigma_{22}}{\sigma_{11}})^3$
$m_1 = m_2$
$\times$ $\frac{m_2}{m_1} = (\frac{\sigma_{22}}{\sigma_{11}})^4$
o $\frac{m_2}{m_1} = (\frac{\sigma_{22}}{\sigma_{11}})^2$

Figure 1

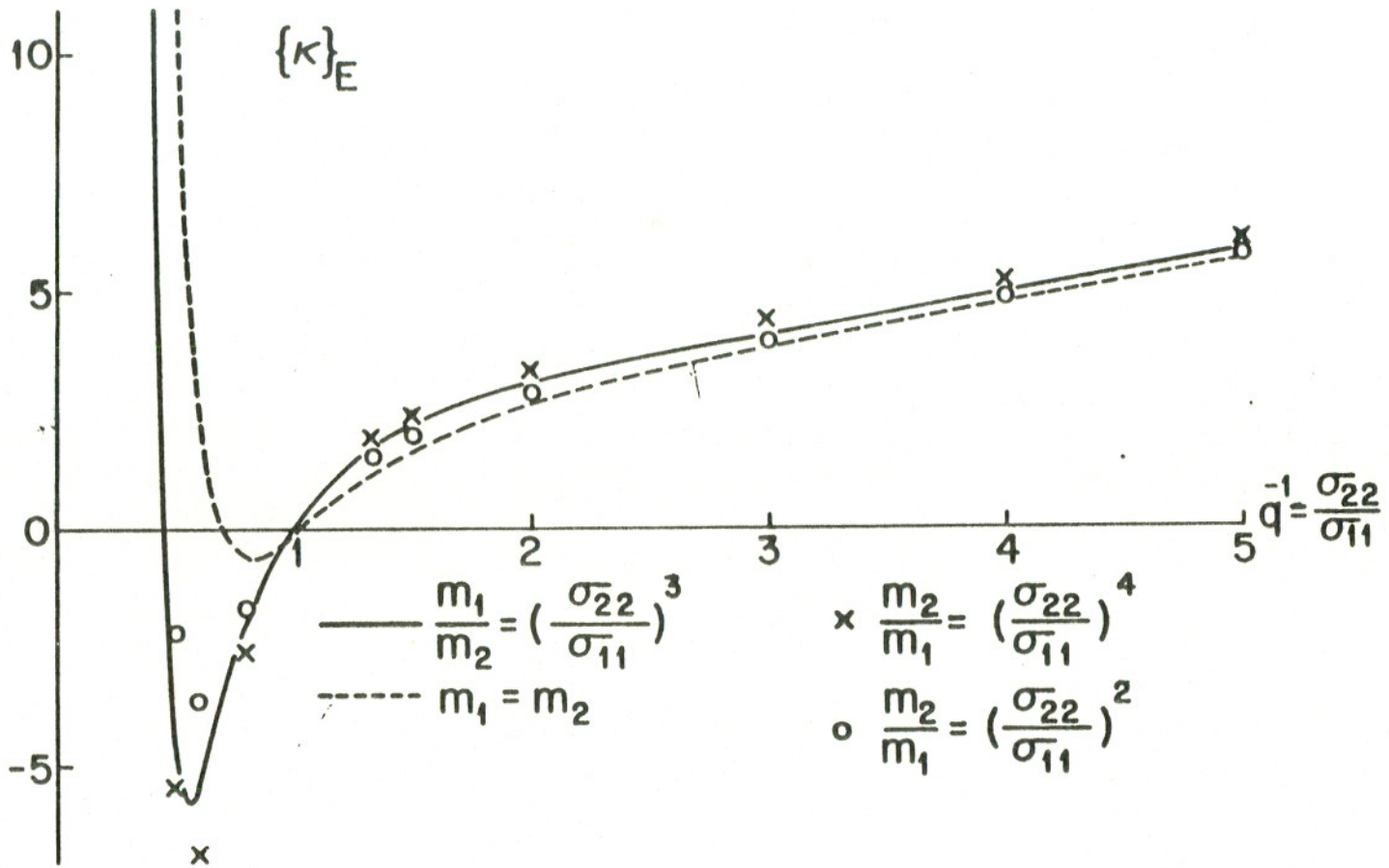
10
5
0
-5
$\{\kappa\}_E$
1
2
3
4
5
$q^{-1} = \frac{\sigma_{22}}{\sigma_{11}}$
$\frac{m_1}{m_2} = (\frac{\sigma_{22}}{\sigma_{11}})^3$
$m_1 = m_2$
$\times \frac{m_2}{m_1} = (\frac{\sigma_{22}}{\sigma_{11}})^4$
$o \frac{m_2}{m_1} = (\frac{\sigma_{22}}{\sigma_{11}})^2$

Figure 2

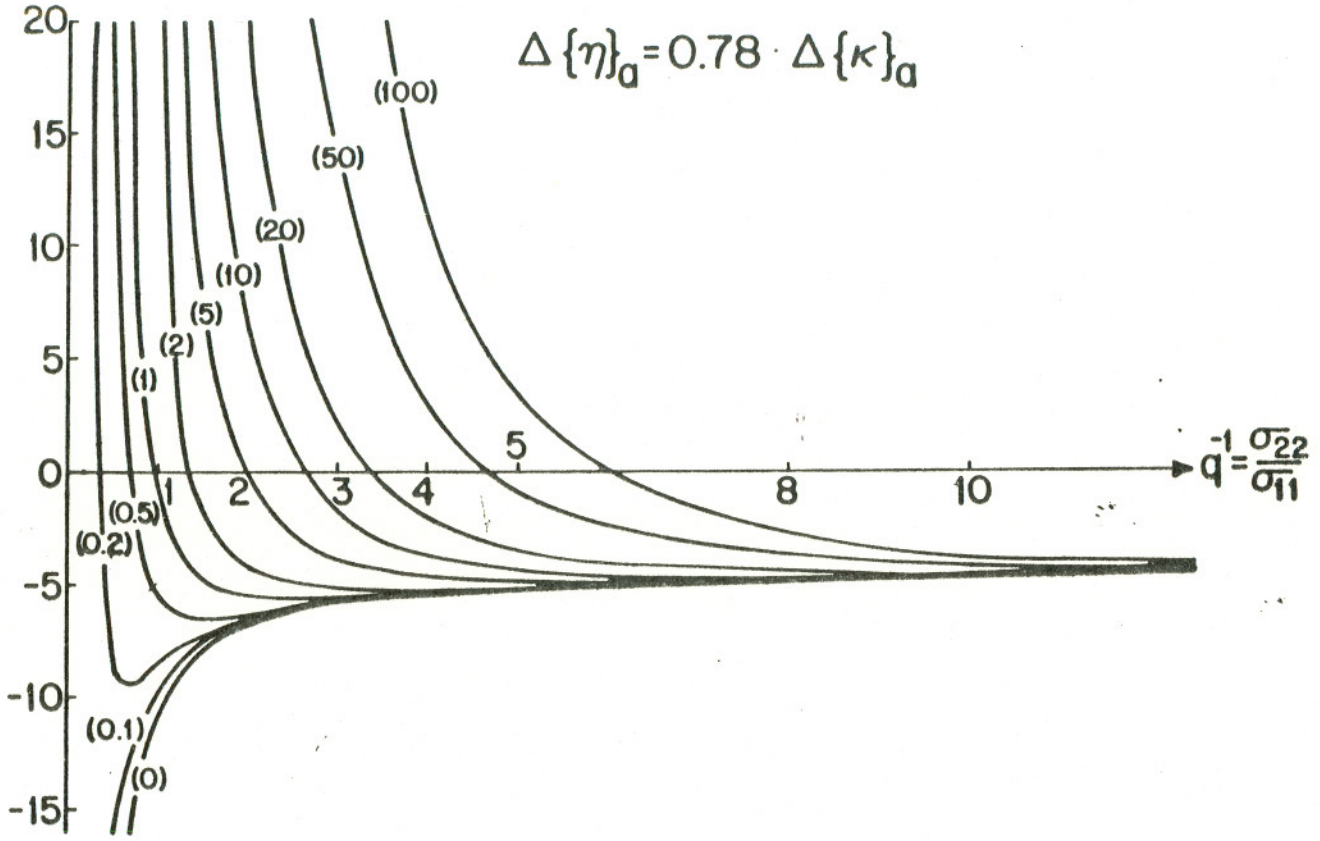
$\Delta\{\eta\}_a = 0.78 \cdot \Delta\{\kappa\}_a$
20
15
10
5
0
-5
-10
-15
(100)
(50)
(20)
(10)
(5)
(2)
(1)
(0.5)
(0.2)
(0.1)
(0)
1
2
3
4
5
8
10
$q^{-1} = \frac{\sigma_{22}}{\sigma_{11}}$

Figure 3

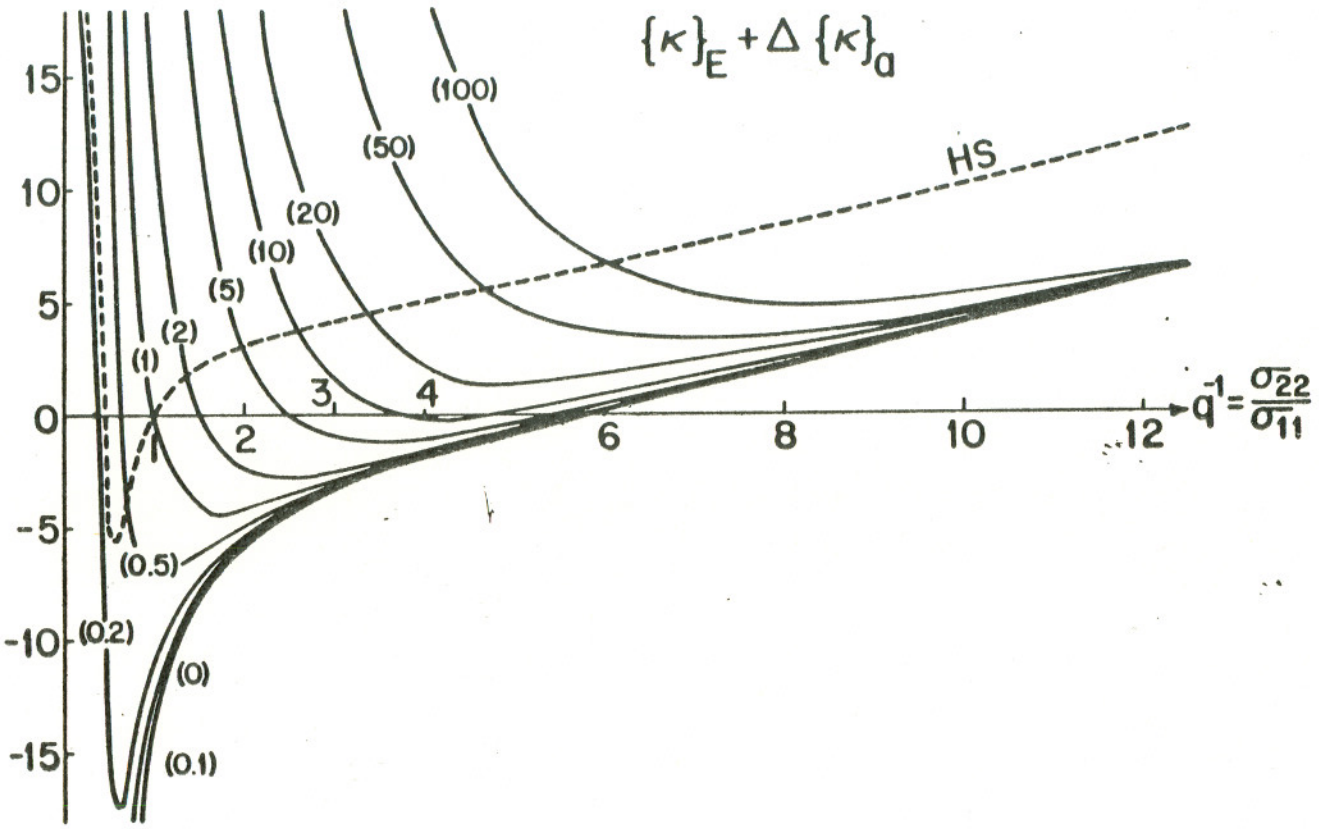
$\{\kappa\}_E + \Delta\{\kappa\}_a$
HS
(100)
(50)
(20)
(10)
(5)
(2)
(1)
(0.5)
(0.2)
(0)
(0.1)
15
10
5
0
-5
-10
-15
2
3
4
6
8
10
12
$q^{-1} = \frac{\sigma_{22}}{\sigma_{11}}$

Figure 5

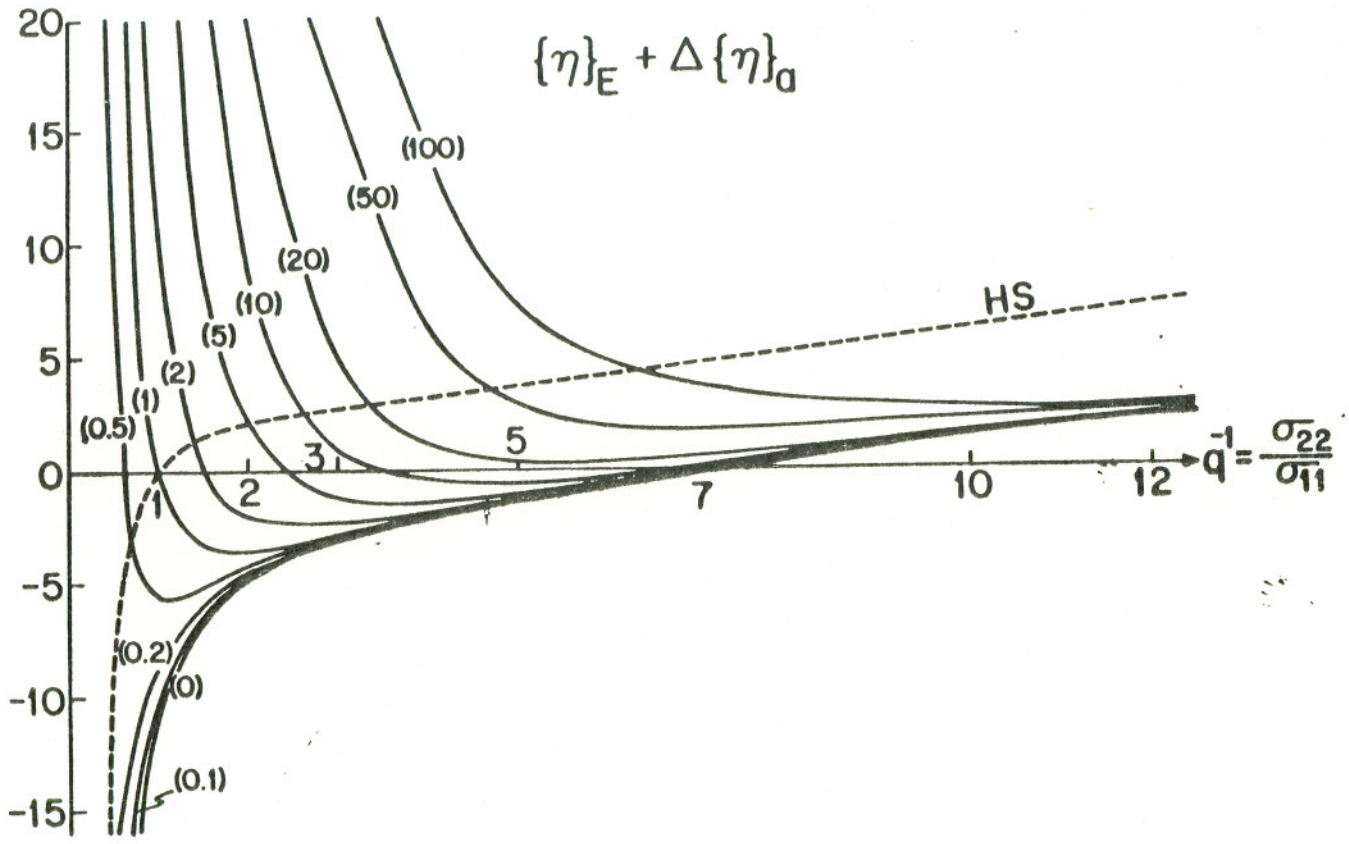
$\{\eta\}_E + \Delta\{\eta\}_a$
20
15
10
5
0
-5
-10
-15
(100)
(50)
(20)
(10)
(5)
(2)
(1)
(0.5)
(0.2)
(0)
(0.1)
HS
1
2
3
5
7
10
12
$q^{-1} = \frac{\sigma_{22}}{\sigma_{11}}$

Figure 4